Beamformer Performance in Sound Fields Produced by Amplitude Panning

Teemu Koski[1], Filippo M. Fazi[2], and Ville Pulkki[1]

[1]*Department of Signal Processing and Acoustics, Aalto University, 02150 Espoo, Finland*

[2]*Institute of Sound and Vibration Research, University of Southampton, Southampton SO17 1BJ, United Kingdom*

Correspondence should be addressed to Teemu Koski (teemu.j.koski@aalto.fi)

ABSTRACT

Increasing motivation to reproduce realistic sound scenes for hearing-instrument users has raised the question whether spatial sound reproduction methods are capable of reproducing sound accurately also for listeners that listen through a hearing instrument with a beamformer. This study presents an analysis of the pressure magnitude errors induced in the output of a beamformer when it is exposed to a sound field produced by amplitude panning. Simulations show that reproduction artifacts are generated by errors in the phase shifts between microphone capsules and due to destructive interference of the sound pressures produced by the reproduction loudspeakers. Using amplitude panning in applications involving listening through beamformers requires the controlling of these sources of errors. It is shown that the adequate loudspeaker span for a given maximum error depends on the directivity of the beamformer in use.

1. INTRODUCTION

The motivation has recently increased to reproduce realistic sound scenes for hearing-impaired listeners and for hearing-instrument users. The developments in hearing instrument technology highlight a need for assessing the real-life benefit given by such devices. Furthermore, reproducing realistic sound scenes in clinical environments can provide means for measuring directly the communication problems faced by aided or unaided listeners. The literature contains several approaches for reproducing realistic sound scenes for this kind of purposes, varying in their reproduction technique, intended use, and complexity [1, 2, 3, 4].

Many of the sound reproduction techniques used in the approaches listed above have been validated for normally-hearing listeners. However, a new challenge is posed to the sound reproduction techniques when the reproduced sound is listened through a hearing instrument instead of an unaided auditory system. Namely, among various other signal processing schemes, modern hearing instruments are typically equipped with a beamformer of some sort. A beamformer typically captures sound simultaneously at multiple spatial locations and combines the signals in such a way that the output level of the beamformer depends on the direction of arrival of the incoming sound. This can be implemented for example with a single multi-port microphone, or with an array of single-port microphone capsules. Consequently, several studies have also attempted to validate reproduction methods specifically from the viewpoint of aided listeners. Subjective evaluation with speech intelligibility tests have been conducted for example in [4, 5]. Objective evaluation for Higher-order Ambisonics in this framework has been addressed in [6].

Compatibility with beamformer-listeners is a relevant question especially in the case of perceptually-motivated sound reproduction techniques, such as amplitude panning techniques and Directional Audio Coding (DirAC [7]), both of which are designed to reproduce the perceptual attributes of sound rather than reproducing the physical sound field accurately. The extent to which these techniques can be used to accurately reproduce spatial sound for listeners who listen through beamformers is currently unclear.

This study analyzes the errors induced in a single beamformer output when it is exposed to a sound field reproduced by a loudspeaker array driven by an amplitude panning algorithm. The aim is to quantify the degree of the error and define the adequate number of loudspeakers needed for a given tolerable error.

2. AMPLITUDE PANNING

Amplitude panning [8] is a technique for controlling the perceived direction of an auditory object between loudspeakers. This auditory object, often referred to as a virtual source, is positioned by adjusting the gain relations of the loudspeakers. Several methods exist for calculating the loudspeaker gains for amplitude panning. With the tangent law, the relation of the loudspeaker gains g_1 and g_2 for stereophonic panning are calculated as

$$\frac{\tan(\gamma/2)}{\tan\beta} = \frac{g_1 - g_2}{g_1 + g_2}, \tag{1}$$

where γ is the loudspeaker span (i.e., the angle between the loudspeakers) and β is the angle of the virtual source, as in Fig. 1. Vector base amplitude panning (VBAP) [9] provides a generalization of the tangent law based on vector algebra. In VBAP, the virtual source is reproduced using a loudspeaker pair (2-dimensional panning) or a loudspeaker triplet (in 3-dimensional panning). In the 2-dimensional case, VBAP and Eq. 1 produce identical loudspeaker gain relations for g_1 and g_2.

3. ANALYSIS OF THE ERROR SOURCES

Figure 1 shows a diagrammatic representation of a two-capsule microphone array exposed to a sound field due to either a real source (left subfigure) or to a virtual source produced by 2-dimensional amplitude panning (right subfigure). The real-source case (case R) is here considered to be the ideal case, which the virtual-source case (case V) tries to emulate. The center point of the microphone array in Fig. 1 is placed on the *reference center point*, which is here defined as the point which is equidistant of the sources/loudspeakers and in which the loudspeaker spans are defined (i.e., the center of the coordinate system).

The sound field produced in case V is different from the field in case R, since the real source is substituted by a virtual source created by two loudspeakers. Consequently, constructive and destructive interference occurs depending on the inspection point, due to summation of the loudspeaker signals with different phase relations. In the reference center point, the interference is always constructive. When moving away from this point to the x-direction (Fig. 1), the phase difference between the loudspeaker signals gradually increases, and eventually the signals cancel out completely due to opposite phase. Moving further, the interference becomes constructive again, thus generating a repetitive pattern of spatially varying magnitude. The

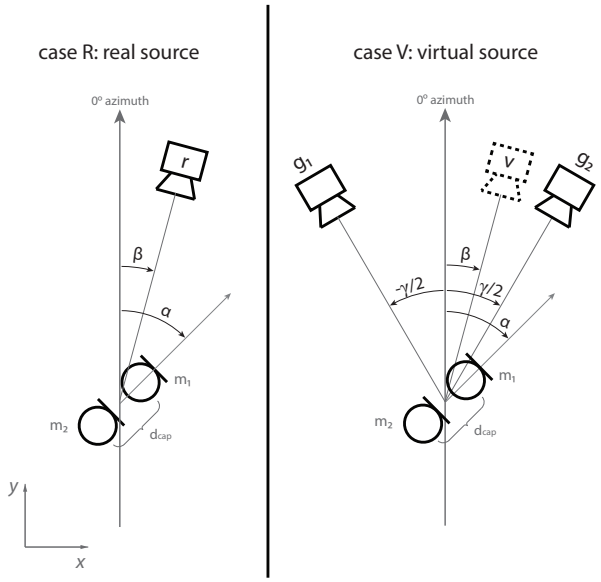

Fig. 1: A two-capsule microphone array listening to a real source (left) and a virtual source produced by amplitude panning with two loudspeakers (right). α – array orientation angle in azimuth; β – real/virtual source position; $\pm\phi/2$ – positions of the reproduction loudspeakers; g_1, g_2 – amplitude panning gains.

distance between the reference center point and the first point where the two signals cancel out can be calculated as

$$d_{\text{int}} = \frac{c}{4f\sin(\gamma/2)}, \tag{2}$$

where c is the speed of sound, f is the frequency, and γ is the loudspeaker span. The microphone capsules are affected by this *destructive interference effect* depending on their position, and this affects the output signal of any beamformer that utilizes the capsule signals.

However, the effect described above may be insignificant when d_{int} is large, microphone array dimensions are low, and the microphone capsules are close enough to the reference center point. Even in this case, another source of error is present. Namely, error is induced by the fact that the phase shift between the microphone capsule points is different in cases R and V. For case R in Fig. 1, if the source was in front of the capsule pair ($\alpha = \beta = 0°$), the phase of a plane wave would shift by $2\pi(d_{\text{cap}}/\lambda)$ radians when propagating from m_1 to m_2. The phase shift is decreased if the array is rotated. Thus, for case R, the

phase shift between m_1 to m_2 is

$$\Delta\phi_r = \frac{2\pi d_{\text{cap}}}{\lambda}\cos(-\alpha+\beta), \tag{3}$$

where d_{cap} is the distance between the capsules, α is the array orientation angle, β is the source angular position, and λ is the wavelength of the reproduced sound. For case V, each loudspeaker poses a different phase shift. If the contribution of each loudspeaker are treated separately, the phase shifts caused by the loudspeaker contributions are

$$\Delta\phi_{LS} = \frac{2\pi d_{\text{cap}}}{\lambda}\cos(-\alpha\pm\gamma/2). \tag{4}$$

That is, the resulting phase shift between the microphone capsules is defined by the phase shifts induced by the loudspeaker contributions. Given that different phase shifts translate to different output magnitudes, this effectively leads to sampling of the beamformer directivity pattern at the reproduction loudspeaker positions – weighted by loudspeaker gains – instead of the real/virtual source position. Consequently, pressure magnitude error is induced in the beamformer output depending on how much the beamformer sensitivity differs for sound coming from the loudspeaker directions compared to sound coming from the source direction. In practice, however, this error induced by the phase shift error is combined with the error induced by the destructive interference effect.

4. SIMULATIONS

Simulations were carried out to quantify the effects analyzed in section 3. Pressure magnitudes in various beamformer outputs were simulated for cases R and V (Fig. 1). In addition, the error for case V in reference to case R was calculated. Simulations were restricted to 2-dimensional panning and for sources located in the horizontal plane.

4.1. Methods

The complex sound pressure $\hat{p}(r,t)$ produced by each source/loudspeaker was calculated as

$$\hat{p}(r,t) = \frac{A_0}{4\pi r}e^{-j\omega t}e^{-jkr}, \tag{5}$$

where A_0 is the source amplitude, r is the distance from the sound source, j is the imaginary unit, t is time, and k is the wave number ($k=\omega/c=2\pi f/c$). The distance from the sources/loudspeakers to the reference center point was set to 10 m.

The complex sound pressure was calculated at the capsule locations of a microphone array, and the magnitude of the beamformer output pressure value was calculated. Figure 2 shows the microphone array and the block diagram for achieving the output sound pressure for beamformers of different orders. The filter $H(f)=c/(j2\pi f d_{\text{cap}})$ compensates for the 90° phase shift and first-order high-pass characteristics caused by the subtraction of two microphone signals. A linear microphone array was chosen to represent a conventional array design in hearing aids. The distance between the microphone capsules d_{cap} was set to 1.6 cm. The zero-azimuth reference points to the middle of the reproduction loudspeaker pair in all simulations (as in Fig. 1).

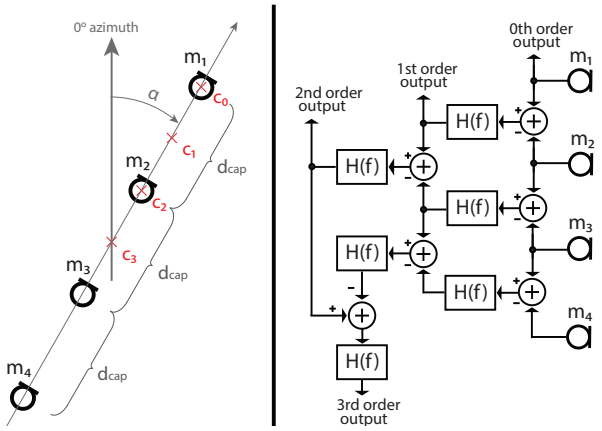

Fig. 2: The linear microphone array used in the simulation (left) and the corresponding block diagram for achieving the beamformer outputs for different orders (right). The points c_0, c_1, c_2, and c_3 are the array center points for respective orders.

The pressure magnitude $P(r)$ in the beamformer output was calculated by taking the absolute value of the complex sound pressure in the output. The sound pressure magnitude error in the beamformer output was calculated in each point as

$$E_{\text{c}}(x,y) = 20\log_{10}\left(\frac{P_{\text{v}}(x,y)}{P_{\text{r}}(x,y)}\right), \tag{6}$$

where (x,y) is the offset of the microphone array center point from the reference center point in x- and y-dimensions, and P_{v} and P_{r} are the pressure magnitudes for cases V and R, respectively. In addition, the average magnitudes ($P_{\text{ra}}(\alpha)$ and $P_{\text{va}}(\alpha)$) and the average magnitude error ($E_{\text{a}}(\alpha)$) were calculated over a listening area. This was done by calculating the root-mean-square values

for P_{ra}, P_{va}, and $(P_{\mathrm{v}}/P_{\mathrm{r}})$ over a range of locations for the microphone array center point[1].

4.2. Results

4.2.1. Orientation-dependent sensitivity for real and virtual sources

Figure 4 presents the microphone-orientation-dependent pressure magnitudes (and related error measures) of the simulated beamformers for real and virtual sources, averaged over an area (radius 0.2 m) around the reference center point. In the case of Fig. 4, the virtual source was panned in the middle of the two loudspeakers for each loudspeaker span ($\beta = 0^\circ$)[2]. First column of subfigures presents $P_{\mathrm{ra}}(\alpha)$, that is, the pressure magnitude as a function of the microphone array orientation for a real source. The second column presents this for a virtual source reproduced with a loudspeaker span of 30°. The third column shows the corresponding pressure magnitude error ($E_{\mathrm{a}}(\alpha)$). The fourth column shows the linear differences in the pressure magnitudes ($D_{\mathrm{a}}(\alpha) = P_{\mathrm{v}}(\alpha) - P_{\mathrm{r}}(\alpha)$). The $P_{\mathrm{r}}(\alpha)$ and $P_{\mathrm{v}}(\alpha)$ can be interpreted as orientation-dependent *sensitivity* patterns for the beamformers for real/virtual sources, and $E_{\mathrm{a}}(\alpha)$ and $D_{\mathrm{a}}(\alpha)$ can be interpreted as two different ways to illustrate the error or difference between the sensitivities for virtual versus real source.

The spatial aliasing frequency of the simulated microphone array is at 10.7 kHz ($f_{\mathrm{alias}} = c/2d_{\mathrm{cap}}$) and this shows in Fig. 4 as deformation of the sensitivity patterns at higher frequencies. Below f_{alias}, the error seems to follow a certain logic[3], as follows. When $\alpha = 0^\circ$, the sensitivity is decreased in all frequencies in case V. In addition, the destructive interference effect is affecting the output increasingly when frequency is increased, and this manifests itself as decreased average magnitude in high frequencies. As α increases, the error decreases. However, around $\alpha = 90^\circ$ (or equivalently in $\alpha = 270^\circ$), where the simulated beamformers ideally have a sensitivity of zero, $E_{\mathrm{a}}(\alpha)$ has a high peak. As the beamformer order increases and the main lobe of the beamformer narrows, the width of this peak widens. In terms of $D_{\mathrm{a}}(\alpha)$, the maximum error happens at $\alpha = 0^\circ$.

[1] That is, the array center point is moved around the reference center point.

[2] Simulations were also done for different panning cases (i.e., β was varied) and it was found out that the largest error was found when $\beta = 0^\circ$.

[3] This was confirmed also for loudspeaker spans of 5–60°.

4.2.2. Magnitude error for sources outside the directivity pattern nulls

Figure 4 indicated that the maximum pressure magnitude error in decibels happens in the cases when the sound source is near the null of the beamformer directivity pattern. Outside of these areas, the error reaches its maximum when $\alpha = \beta = 0^\circ$, given that the signal frequency is below the microphone array spatial aliasing frequency. Thus, to analyze the maximum direction-dependent error outside the nulls of the beamformer directivity pattern, the pressure magnitude error was calculated in the case $\alpha = \beta = 0^\circ$. Figure 5 presents this error for different beamformer orders and different loudspeaker spans. Left subfigures show the error when the microphone array center is in the reference center point, and the right subfigures show the error averaged over an area around the center (radius 0.2 m).

The left subfigures in Fig. 5 indicate that when the microphone array is in the center, the error is by much independent of frequency up to f_{alias}. The simulation was repeated with different values of d_{cap}, and the frequency where the error crosses the 0 dB-line seemed to follow f_{alias}. When the error is averaged over a listening area (right subfigures in Fig. 5), the error depends more on frequency. As the frequency increases, the listening area is increasingly affected by the destructive interference effect. In Fig. 5e, which shows the error in the omnidirectional microphone output, the error is completely due to the destructive interference effect. When the microphone order increases (Figs. 5f, 5g, and 5h), this effect is added by the frequency-independent error that could be seen already in Figs. 5b, 5c, and 5d. In fact, the averaged errors on the right of Fig. 5 could be precisely replicated by simply summing the error shown in Fig. 5e with the center-errors shown on the left of Fig. 5.

5. DISCUSSION

5.1. Contribution of the error sources

The simulations suggested that the pressure magnitude error induced in the beamformer output depends on the loudspeaker span, the beamformer order, source direction, the microphone array dimensions, and the distance of the microphone array from the reference center point (d_{cent}). Microphone array dimensions are quantified by the distance between the furthest capsules d_{arr} and the distance between the closest capsules d_{cap}. Three mechanisms of error induction have been identified:

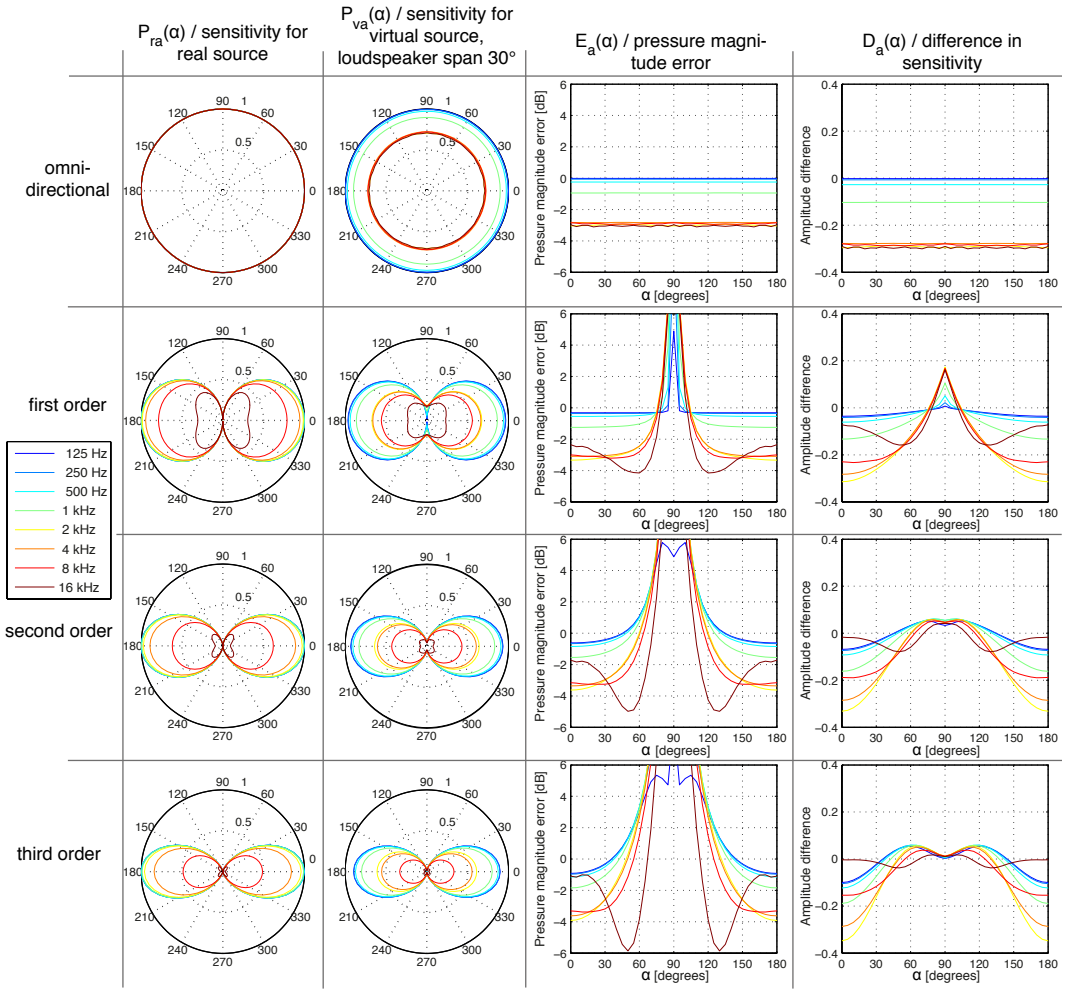

Fig. 4: Comparison of the orientation-dependent pressure magnitudes (or sensitivities) of the simulated beamformers for real and virtual sources. First column – pressure magnitude produced by a real source, second column – pressure magnitude produced by a virtual source with 30-degree loudspeaker span, third column – pressure magnitude error, fourth column – subtraction of the pressure magnitudes (virtual minus real). The errors for microphone orientation angles $\alpha = 180°...360°$ are identical to errors for $\alpha = 0°...180°$. Values are averaged over an area around the reference center point (radius 0.2 m).

1) Phase gradient error. When $d_{\text{cent}} \ll d_{\text{int}}$ and $d_{\text{arr}} \ll d_{\text{int}}$, the error is due to error in the phase shift between the microphone capsules. This error seems not to be frequency dependent, but occurs also in the reference center point, and increases with beamformer order. It was noticed that for the microphone arrays used in the simulation this error component is given by

$$E_{\text{max-dif}} = 20\log_{10}(\cos^N(\gamma/2)), \qquad (7)$$

when $\alpha = \beta = 0°$. This is logical, since the directivity patterns of the beamformers used in this study ideally follow the form $\cos^N \alpha$, and as discussed in Section 3, the error in the reference center point occurs due to sampling of the microphone directiv-

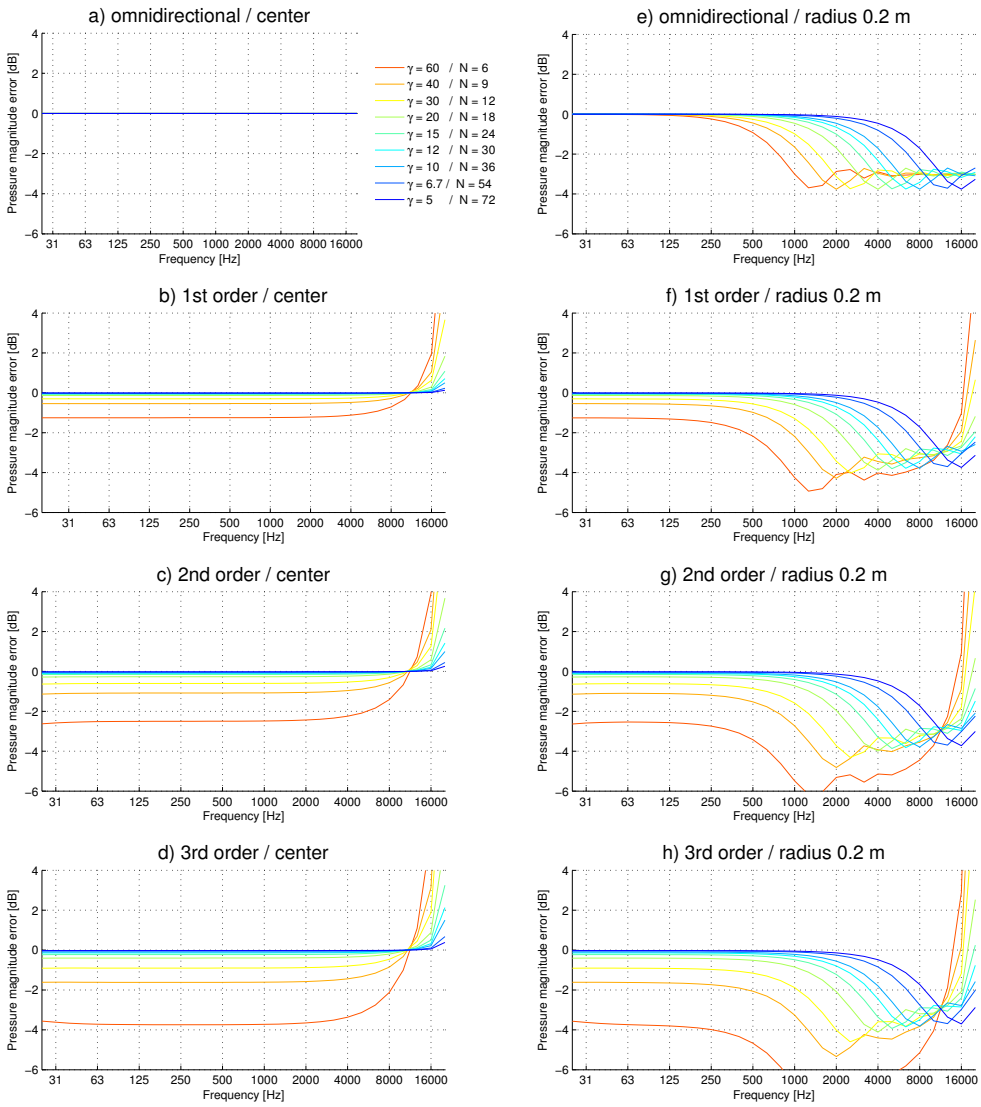

Fig. 5: Pressure magnitude errors for different microphone orders in different reproduction setups (γ = loudspeaker span, N = number of loudspeakers in equiangular horizontal loudspeaker setup). The source is in front of the beamformer ($\alpha = 0°$) and the virtual source is panned in the middle of the loudspeakers ($\beta = 0°$). Left subfigures show the error when the microphone array center point is in the reference center point. Right subfigures show the error averaged over an area around the reference center point (radius 0.2 m).

ity pattern at loudspeaker positions instead of the real/virtual source position.

2) *Interference.* When d_{cent} is comparable with d_{int}, the destructive interference effect starts to affect the overall magnitude response of the microphone output. That is, position-dependent attenuation occurs in a narrow frequency range. This phenomenon takes the form of a high-shelving attenuation in the spatially-averaged error visualizations of Figs. 5e, 5f, 5g, and 5h. Since d_{int} depends on frequency and loudspeaker span, the frequency above which this phenomenon

takes place depends on the loudspeaker span.

3) *Aliasing.* When d_{cap} is comparable with d_{int}, the sensitivity pattern is deformed, because different capsule signals are affected differently by the destructive interference. According to Fig. 5, it seems that this mechanism does not result in an increase of error at frequencies lower than the microphone array spatial aliasing frequency. From Fig. 4 it can be noticed that for the 30° loudspeaker span, the sensitivity patterns are deformed in the high frequencies. The patterns are deformed in the real-source case as well, due to spatial aliasing, but the resulting aliased pattern seems to be different in the real-source case and the virtual-source case. That is, when approaching f_{alias}, the sensitivity pattern in the virtual-source case is affected not only by the aliasing which occurs also in the real-source case but also by an additional aliasing factor caused by the destructive interference effect. Thus, the error in the frequency range close to and above of f_{alias} is not easily described and can be specific to the microphone array layout.

5.2. Relevance of the errors

The interpretation of the effect of the destructive interference arising in amplitude panning is a central element to be considered when evaluating the relevance of the errors identified by the simulations. With reference to Fig. 4 and the right subfigures of Fig. 5, it is important to assimilate that wide-band high-frequency attenuation occurs only when averaging over a listening area. In a single point, the effect of destructive interference influences only in a narrow frequency range. When the inspection point is moved in space, this dip in the magnitude spectrum occurs at a different frequency. The situation is more complex in real-life listening scenarios, where a listener is located in a real room and is wearing a hearing instrument where the microphone array is mounted. When the loudspeakers are in a real room, the effect of the destructive interference is less significant as room reflections are summed to the resultant sound pressure field. Also, if the listener uses both ears, the magnitude response dip is different in the two ears. The spectral coloration of virtual sources in amplitude panning is discussed in more detail in [10].

Another central element to be considered is the interpretation of the large pressure magnitude error (in dB-scale) that occurred in cases where the source was located at a angular position close to a null in the beamformer directivity pattern. The relevance of this kind of error might be low in real-life applications described above, if the resulting directivity pattern of the hearing aid and the head has no distinct null. However, the analysis of this aspect is left for further research, and the further analysis in this report is conducted outside of the angular zone in close proximity of the beamformer directivity pattern nulls.

5.3. Error due to beamformer directivity

If the effects of amplitude panning for omnidirectional sensors are neglected, the error in the beamformer output is dependent only on the shape of the beamformer directivity pattern, source direction, and the loudspeaker span[4]. In Section 4.2.2 it was noted that the averaged-error curves on the right of Fig. 5 could be precisely replicated by simply summing the error seen in Fig. 5e with the errors seen in Figs. 5a–d. That is, for case $\alpha = 0°$, below the spatial aliasing frequency, the additional error caused by increasing beamformer order (compared to 0th order) equals the frequency-independent center-error seen in the left-side subfigures of Fig. 5. This additional error could also be calculated with Eq. (7) for beamformers with directivity patterns of type $\cos^N \alpha$. The generalized form of this equation would be

$$E_{\text{max-gen}} = 20\log_{10}(B(\gamma/2)), \tag{8}$$

where B is the directivity pattern function for the beamformer.

Although no proof for Eq. (8) is given here, the simulations described earlier in this report were repeated for a set of figure-of-eight beamformers ($B = \cos^N \alpha$) and circular harmonic beamformers ($B = \cos(N\alpha)$) for orders $N = 1...5$. For the figure-of-eight, similar linear array layout was used as in Fig. 2, with N+1 microphone capsules. For the circular harmonic beamformer, a circular array layout with $2N+1$ microphone capsules was used. The simulation results showed that the observations stated in Section 5.1 could be extended to these beamformers as well, and Eq. (8) accurately defined the error induced by the beamformer directivity when $\alpha = \beta = 0°$. Furthermore, the behavior of the error as function of α followed the same logic as seen in Fig. 4 and as discussed in Section 4.2.1.

Based on these results, it can be concluded that below f_{alias}, Eq. (8) can be used to define the error due to beamformer directivity in sound fields produced with amplitude panning (compared to an omnidirectional sensor)

[4] Given that the signal frequency is below the microphone array spatial aliasing frequency.

for sources in the front ($\alpha = 0°$). Additionally, this error represents the maximum error for the whole range of α excluding the areas at close proximity of beamformer directivity pattern nulls. This is true at least for the microphone arrays used in the simulations. Table 1 shows the maximum loudspeaker spans for each simulated beamformer, given that a maximum of 1 dB error for sources outside the directivity pattern nulls is tolerated compared to an omnidirectional sensor. The table also shows the corresponding minimum numbers of loudspeakers for full equiangular horizontal loudspeaker setup. The values were calculated with Eq. (8) and verified with simulations described above.

Beamformer type and directivity pattern	Order (N)	Maximum loudspeaker span	Minimum number of loudspeakers
Figure-of-eight $\cos(\alpha)^N$	1	53.9°	7
	2	38.5°	10
	3	31.5°	12
	4	27.4°	14
	5	24.5°	15
Circular harmonic $\cos(N\alpha)$	1	53.9°	7
	2	27.0°	14
	3	18.0°	20
	4	13.5°	27
	5	10.8°	34

Table 1: Maximum loudspeaker spans for amplitude panning for different types of beamformers that listen to the reproduced sound: 1 dB maximum direction-dependent pressure magnitude error compared to omnidirectional sensor is tolerated. The error is defined for sources with angular position outside the close proximity of the nulls of the beamformer directivity pattern. Minimum number of loudspeakers refer to a full equiangular setup in the horizontal plane that corresponds to the loudspeaker span.

6. CONCLUSIONS

An analysis has been presented of the source-direction-dependent sound pressure magnitude errors induced in a beamformer output when it is exposed to a sound field reproduced by amplitude panning. Depending on the loudspeaker span and the signal frequency, any microphone input is affected by the destructive interference of the sound fields produced by the loudspeakers. In addition, error in phase gradient at the microphone inputs causes pressure magnitude error in the beamformer output, depending on source direction, loudspeaker span, and the beamformer directivity. The results of this study suggest that amplitude panning can be used for applications involving listening through beamformers if the sources of errors are successfully controlled: the adequate loudspeaker span for a given maximum error depends on directivity/order of the beamformer in use. This study defined the errors for two beamformer types with different orders, for which the corresponding loudspeaker-setup criteria are given in Tab. 1.

7. ACKNOWLEDGEMENTS

The Academy of Finland has supported this work. The research leading to these results has received funding from the European Research Council under the European Community's Seventh Framework Programme (FP7/2007-2013) / ERC grant agreement no [240453].

8. REFERENCES

[1] S. Favrot and J. M. Buchholz, "LoRA: A Loudspeaker-Based Room Auralization System," *Acta acustica united with Acustica*, vol. 96, pp. 364–375, March/April 2010.

[2] L. J. Revit, M. C. Killion, and C. L. Compton-Conley, "Developing and Testing a Laboratory Sound System That Yields Accurate Real-World Results," *Hearing Review*, October 2007.

[3] P. Minnaar, S. F. Albeck, C. S. Simonsen, B. Søndersted, S. A. D. Oakley, and J. Bennedbæk, "Reproducing Real-Life Listening Situations in the Laboratory for Testing Hearing Aids," in *AES 135th Convention*, (New York, NY, USA), October 2013.

[4] T. Koski, V. Sivonen, and V. Pulkki, "Measuring Speech Intelligibility in Noisy Environments Reproduced with Parametric Spatial Audio," in *AES 135th Convention*, (New York, NY, USA), October 2013.

[5] J. Cubick, S. Favrot, P. Minnaar, and T. Dau, "Validation of a Virtual Sound Environment System for Hearing Aid Testing," in *AIA/DAGA Conference on Acoustics*, (Merano), March 2013.

[6] C. Oreinos, J. M. Buchholz, and J. Mejia, "Effect of Higher-Order Ambisonics on Evaluating Beamformer Benefit in Realistic Acoustic Environments,"

in *IEEE Workshop on Applications of Signal Processing to Audio and Acoustics*, (New Paltz, NY, USA), October 2013.

[7] V. Pulkki, "Spatial Sound Reproduction with Directional Audio Coding," *Journal of Audio Engineering Society*, vol. 55, pp. 503–516, June 2007.

[8] A. D. Blumlein, "British Patent Specification 394,325," *J. Audio Eng. Soc.*, vol. 6, pp. 91–98, April 1958.

[9] V. Pulkki, "Virtual Source Positioning Using Vector Base Amplitude Panning," *J. Audio Eng. Soc.*, vol. 45, pp. 456–466, June 1997.

[10] V. Pulkki, "Coloration of Amplitude-Panned Virtual Sources," in *AES 110th Convention*, (Amsterdam, The Neatherlands), May 2001.